Experimental Mechanics (2010) 50:491–499
DOI 10.1007/s11340-009-9254-5

High Temperature Nanoindentation of PMR-15 Polyimide

Y.C. Lu · D.C. Jones · G.P. Tandon · S. Putthanarat · G.A. Schoeppner

Received: 13 July 2008 / Accepted: 8 May 2009 / Published online: 27 May 2009

Abstract This paper presents the high temperature nanoindentation experiments performed on an aerospace polymer resin–PMR-15 polyimide. The sharp-tipped Berkovich nanoindenter equipped with a hot-stage heating system was used. The indentation experiments were performed using the "hold-at-the-peak" method at various indenter holding times and unloading rates. The creep effect was seen to decrease with increasing holding time and/or unloading rate. Procedures used to minimize the creep effect are investigated at both ambient and elevated temperatures so that the correct contact depth (together with modulus and hardness) can be determined from nanoindentation load-depth curve. The temperature dependent mechanical properties of PMR-15 are measured through the current nanoindenter and results are consistent with those obtained from macroscopic tests.

Keywords Nanoindentation · High temperature · PMR-15 polyimide · Viscoelastic creep

Y.C. Lu (✉) · D.C. Jones
University of Kentucky,
Lexington, KY, USA
e-mail: chlu@engr.uky.edu

G.P. Tandon (SEM member) · S. Putthanarat · G.A. Schoeppner
Air Force Research Laboratory,
Materials and Manufacturing Directorate, AFRL/RXBC,
Wright Patterson AFB,
Dayton, OH, USA

G.P. Tandon · S. Putthanarat
University of Dayton Research Institute,
Dayton, OH, USA

Introduction

The nanoindentation technique has been well recognized as a small scale test for characterizing the mechanical properties of materials in small dimensions or in localized regions. It employs high-resolution actuators and sensors to continuously control and monitor the loads and displacements on an indenter as it is driven into and withdrawn from a material. From the load-depth response, many useful engineering properties can be extracted, including the static properties such as modulus, yield strength, and fracture toughness [1–7] and the viscoelastic properties such as creep and stress relaxation [8–10]. However, the nanoindentation technique is currently limited to measuring the mechanical properties at ambient temperature. Several technical issues exist surrounding the use of nanoindentation at elevated temperatures, including (1) thermal equilibration of samples and instrument, (2) instrumental drift at high temperatures, and (3) temperature-induced changes to the indenter tip function (indentation area function).

Only a scant amount of literature is available addressing the use of high temperature nanoindentation and the work has been limited to linear, elastic materials [11–14]. Beake and Smith are the first to report the high temperature nanoindentation experiments [11]. The tests were conducted on fused silica and soda-lime glass and the modulus and hardness measured up to 400°C. Schuh et al. [12] has recently conducted a comprehensive study on high temperature nanoindentation on fused silica. Significant modification has been made on the nanoindenter equipment to address fundamental issues related to the high temperature nanoindentation such as thermal drift and machine equilibrium. Volinsky et al. [13] and Sawant and Tin [14] have

recently reported the uses of high temperature nanoindentation on characterizing the mechanical properties of hard thin films and single crystal super-alloys.

All these high-temperature nanoindentation works have been limited to the hard materials (ceramics and super-alloys). In the present study, the high temperature nanoindentation tests were performed on a relatively softer material–PMR-15 polyimide. PMR-15, prepared by polymerization of monomeric reactants, has been widely used as the matrix resins in fiber-reinforced composites for various aerospace high temperature applications. Thermo-oxidative degradation of polymer matrix composites is clearly a subject of major importance as designers push the high temperature endurance limits of polymer composites to improve the performance of aerospace systems. The high temperature aging behavior of PMR-15 resin has been studied by a number of authors [15]. Using optical microscopy and nanoindentation techniques, it has been reported [16] that for PMR-15 polymer degradation occurs within a thin surface layer that develops and grows during thermal aging. Evidence for changes occurring on the aged sample surface has been further provided by microscopic FT-IR [17]. The FT-IR spectra and indentation measurements also indicated that no changes whatsoever occurred in the interior of PMR-15 specimens aged for hundreds of hours at elevated temperatures. In the present experiments, the *unaged* PMR-15 neat resin was characterized using a nanoindenter equipped with a hot-stage heating system. The objective is to develop a reliable testing and analysis methodology for measurement of temperature-dependant mechanical properties using high-temperature nanoindentation technique.

Experimental Technique

Materials

Rectangular PMR-15 neat resin plaques were compression molded by Hycomp Inc.(Cleveland, OH) according to the manufacturer's suggested cure cycle [18] and subsequently post-cured in air for 16 h at 316°C[1]. Smaller specimen (100 mm×100 mm×2 mm) was subsequently cut from the plaque using a diamond saw with distilled water as a cooling media. The specimen was washed using a common household soap and then rinsed with distilled water for a minimum of 5 min. Rubber gloves were worn throughout while handling the sample in order to prevent contamination of specimens from oils, etc. The specimen was then dried with standard paper towels and placed in a vacuum oven at 105°C for a minimum of 48 h to remove any moisture within the samples, and stored in a nitrogen purged desiccator until testing. The specimen was then potted in Jeffamine 828-D230 epoxy resin that was cured at room temperature for 3 days. The surface of the specimen was prepared by grinding papers and polishing compounds, the final polishing compound being alumina with an average particle size of 0.3 μm. The potted specimen was used for surface profiling, optical microscopy measurements and nanoindentation testing.

Equipment

The high-temperature nanoindentation tests were performed on a Nano Indenter XP equipped with thermal control system (MTS NanoInstruments, Oak Ridge, TN). The thermal control system consists primarily of (a) a hot-stage assembly positioned below the test specimen, (b) a stainless steel heat shield that is used to isolate the indenter transducer assembly from the heat source, (c) a coolant system that is used to remove heat from the surrounding stage, and (d) a temperature controller. The hot-stage assembly is an aluminum stage holder containing a resistance-type microheater, a coolant port and a ceramic isolator. The temperature of the hot-stage can be set up to 400°C by using an electronic controller and monitored by a LabView data acquisition system through a J-type thermocouple embedded inside the hot-stage. The PMR-15 specimen was mounted to a special sample disk using a high-temperature adhesive (Poly-2000). This adhesive is designated for extreme temperature applications, up to 1,090°C, and possesses a minimum amount of thermal expansion.

The Berkovich diamond indenter was used in the present experiments. The indenter has a nominal tip radius <20 nm and an inclined angle of θ=65.3°. The latest tips provided by the manufacturer had all been brazed onto the tip holder, a process allowing tips to be used at elevated temperatures. The entire tip assembly was attached directly to the force transducer which is behind the installed heat shield. To minimize the distribution of heat into the entire testing system, the specimen (mounted on the hot-stage) was heated outside the machine and then brought in contact with the indenter tip. As the hot specimen was in contact with a cold tip, rapid heat transfer occurred. Additional time (~60 min.) was given for redistribution of heat to ensure the indenter-specimen system equilibrated at the given test temperature. The thermal drift rate used was 0.1 nm/s. After each temperature experiment, the tip was cleaned to ensure that it was not contaminated by heated polymer samples. The applied load and penetration depth were recorded during each test and used to compute the modulus and hardness of the materials.

[1] The post-cure temperature was incorrectly stated as 343°C in [16, 25]

Data Analysis

Polymers exhibit time-dependent viscoelastic deformation, i.e., creep, particularly at elevated temperatures. It is known that during the nanoindentation of a viscoelastic material, the resultant load–displacement plot may exhibit a "nose" (or a "bulge") in the initial unloading segment due to excessive creep. When a "nose" occurs, the resultant contact stiffness will be negative [19–22]. To reduce the creeping effect (as well as other effects such as instrument drift) on the unloading set of data, a technique called "held-at-the-peak" has been recently adopted for nanoindentation testing of polymers [19–22]. That is, the indenter is held at the maximum load for a length of time prior to unloading, a procedure allowing the material to relax and provoking the disappearance of the "nose". Once the apparent "nose" is eliminated from the initial unloading curve, the elastic contact depth can be estimated from the indentation load-depth curve through a modified Oliver-Pharr equation [22]

$$h_c = \left(h_{max} - h_{creep}\right) - 0.75\frac{P_{max}}{S_e} \tag{1}$$

where h_{max} is the maximum indentation depth and h_{creep} the change in the indentation depth during the holding time. P_{max} is the peak load and S_e the elastic contact stiffness. According to Ngan and Tang [19], the total displacement under the indenter at the moment of unloading can be decomposed into elastic component (h_e) and creep component (h_v), based on a simple spring-dashpot model. Thus, the elastic contact stiffness (S_e) can be determined from the apparent stiffness (S) as follows [19]

$$\frac{1}{S} = \frac{\partial h}{\partial P} = \frac{\partial(h_e + h_v)}{\partial P} = \frac{\partial h_e}{\partial P} + \frac{\dot{h_v}}{\dot{P}} = \frac{1}{S_e} + \frac{\dot{h_v}}{\dot{P}} \tag{2a}$$

or

$$\frac{1}{S_e} = \frac{1}{S} - \frac{\dot{h}_v}{\dot{P}} \tag{2b}$$

where S is the apparent stiffness that is determined from the slope of the unload curve evaluated at the maximum depth $\left(S = (dP/dh)_{h=h_{max}}\right)$. $\dot{h_v}$ is the creep rate at the end of the load hold and $\dot{P}$ the unloading rate. Substituting equation (2b) into equation (1), the correct contact depth is determined by

$$h_c = \left(h_{max} - h_{creep}\right) - 0.75P_{max}\left(\frac{1}{S} - \frac{\dot{h}_v}{\dot{P}}\right) \tag{3}$$

Once the correct contact depth is known, the indenter-sample contact area (A) can be estimated through a tip-area function. The tip-area function is an experimentally determined function of the contact depth, h_c, expressed as follows

$$A = C_0 \cdot h_c^2 + \sum_{i=1}^{n} C_i \cdot h_c^{1/2^i},\ n = 8 \text{ or less} \tag{4}$$

where C_0 and C_i are coefficients determined through a calibration process on reference materials (high-purity fused silica) provided by the MTS. The first term (C_0) would be the area versus contact depth for a perfectly sharp Berkovich indenter while the following terms (C_i) account for tip bluntness.

After estimating the indenter-sample contact area (A), the elastic modulus (E) and hardness (H) can be calculated following the standard procedures [5, 6]

$$E = \frac{1 - \nu^2}{\frac{1}{E_r} - \frac{1-\nu_i^2}{E_i}} \tag{5}$$

$$H = P_{max}/A \tag{6}$$

where $E_r = \frac{\sqrt{\pi}}{2\cdot(1.034)}\frac{S_e}{\sqrt{A}}$ and E_i and ν_i are the elastic modulus and Poisson's ratio of the indenter (for diamond indenter: E_i=1,140 GPa and ν=0.07).

Results and Discussion

Creep Effect in Nanoindentation of Polymers

PMR-15 is a thermoset polymer and known to exhibit viscoelastic creep, particularly at elevated temperatures. The standard nanoindentation test is based on the assumption that the deformation during initial unloading is purely elastic. Thus, by curve-fitting the slope of the initial unloading curve, the elastic contact stiffness (S_e) can be computed, from which the contact depth (h_c) and elastic modulus (E) are calculated [5, 6]. When indenting a material exhibiting time-dependent deformation, errors may occur in determining the contact stiffness and contact depth using the same method (due to the presence of viscoelastic creep at the initial unloading). To minimize the creep effect, the present experiments were performed using the "hold-at-the-peak" method, a procedure proposed by some researchers for indenting viscoelastic materials [19–22]. In the tests, the indenter was loaded at a maximum load, held at the peak for a length of time and then unloaded. Various indenter holding times and unloading rates were used to investigate the creep effect.

Figures 1(a), (b) and (c) show the indentation load-depth responses of PMR-15 at ambient temperature (T= 23±0.5°C). In each test, the PMR-15 specimen was indented using the "hold-at-the-peak" method under

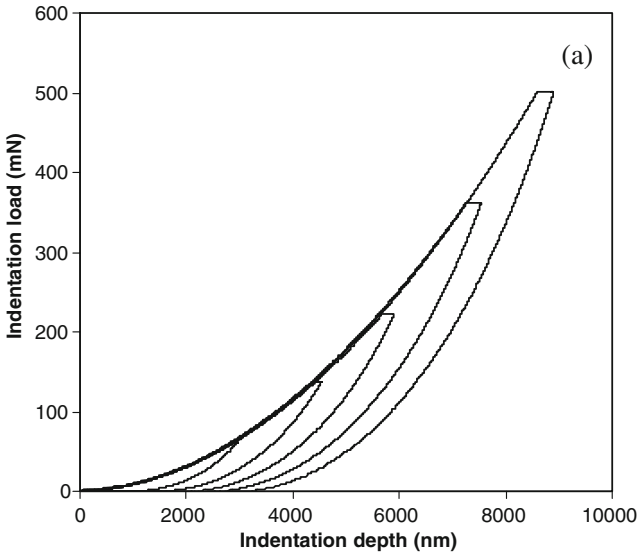

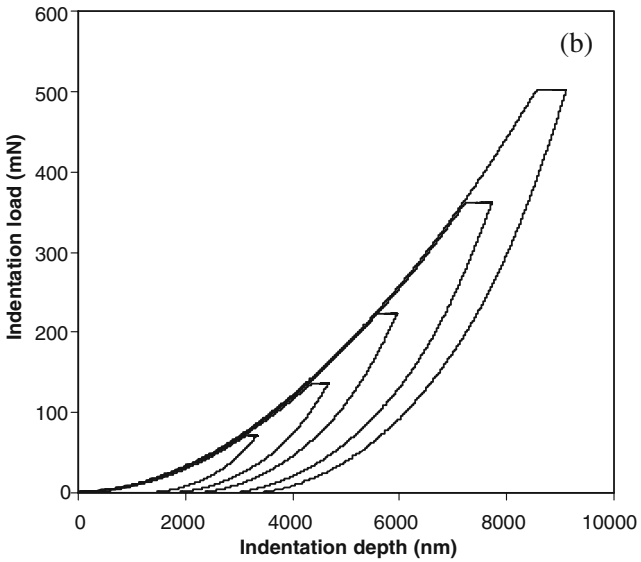

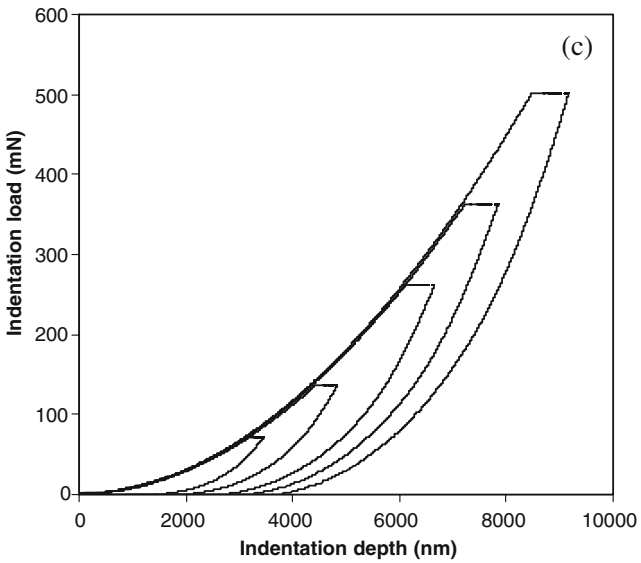

◀ **Fig. 1** Indentation load-depth curves of PMR-15 polyimide with a holding time of (**a**) 2 s, (**b**) 20 s, and (**c**) 120 s

increased load up to a maximum of 500 mN. The holding time in Fig. 1(a), (b) and (c) is 2 s, 20 s, and 120 s, respectively. It is observed that while held at constant load, the indenter continues to penetrate into the specimen, an indication that the present PMR-15 material undergoes creep deformation even at ambient condition. For comparison, the high purity fused silica, a linear elastic material, was tested under the same conditions (with holding times of 2 s, 20 s and 120 s). As an example, the load-depth curves under a 20 s holding time are shown in Fig. 2. It is seen that no visible creep has occurred on fused silica, which is consistent with the results reported by Beake and Smith [11].

As the holding time increases from 2 s to 120 s, the creep distances increase as expected [Fig. 1(a), (b), (c)]. The amount of creep also increases with the increase of indentation load, as seen in Fig. 1(a), (b), (c). To better illustrate the creep effect, Fig. 1(b) is re-plotted by showing the indenter displacement at each holding-time segment (Fig. 3). The plots show that the indentation displacement increases rapidly at the initial holding time, then stabilizes at longer holding time, an indication that a quasi-steady flow state may have reached in the material. From these creep plots, the indentation creep rates during holding period can be calculated by $\dot{h}_v = \partial h_v/\partial t$ [23, 24]. In this paper, the indentation creep rate, $\dot{h}_v$, was normalized with the indenter unloading rate, $\dot{P}$, where $\dot{P} = \partial P/\partial t$. The normalized creep rate ($\dot{h}_v/\dot{P}$), the third term in equation (3), can be viewed as a "creep factor" during the indentation of

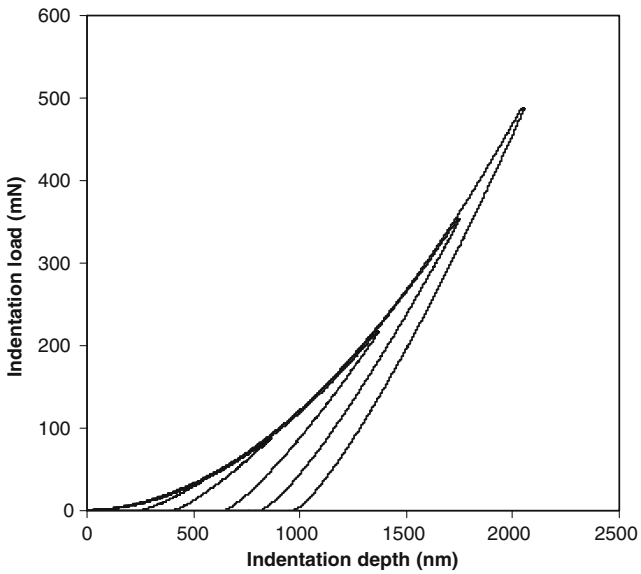

Fig. 2 Indentation load-depth curves of fused silica with a holding time of 20 s

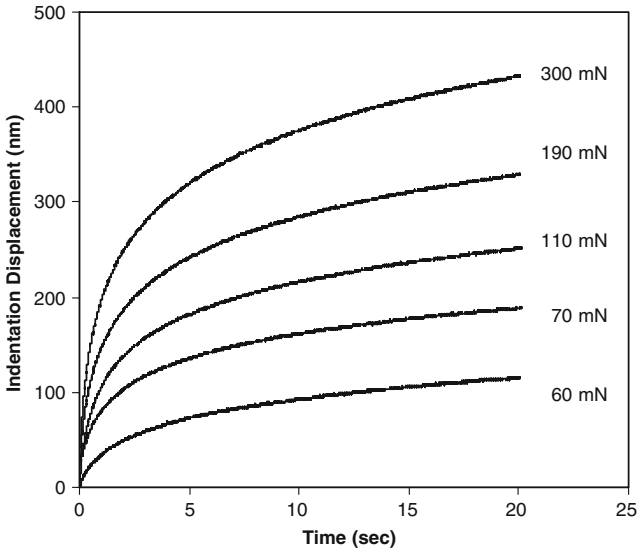

Fig. 3 Creep response of PMR-15 during holding period. This figure is a re-plot of the holding-time segments in Fig. 1(b)

polymeric materials. It is seen that a small creep factor would require a long load-hold period and/or a fast indenter unloading rate.

The normalized indentation creep rates ($\dot{h}_v/\dot{P}$) of the present PMR-15 were calculated, based on the results shown in Fig. 3. Overall, the indentation creep rates, or the creep factors, are higher at the beginnings of the indenter holding period and then decrease with increasing the holding time (Fig. 4). The creep factor is also affected by the indenter unloading rate $(\dot{P})$. The larger the $\dot{P}$, the smaller the creep effect. For the present highly cross-linked PMR-15 polyimide, the creep factor has become negligibly small at longer holding time. These experimental results are consistent with a recent study by Cheng and Cheng [21]. They conducted the finite element simulation on nanoindentation of viscoelastic materials and found that the contact stiffness obtained from the initial unloading response may be affected by the indenter holding history and initial unloading condition. An indenter hold period is necessary to minimize the creep effect occurred at the onset of indenter unloading. The creep effect can also be reduced by using a fast unloading rate.

Various indenter holding times have been used in the present PMR-15 experiments, ranging from 0.1 to 120 s (Fig. 5). From the initial unloading responses, the elastic contact stiffness (S_e) was calculated as a function of holding time, via equation (2b). As seen in Fig. 6, S_e remains relatively unchanged at longer holding times (as $t>$ 1 s). Similar results have been reported by other researchers [20, 22]. For example, Briscoe et al [20] has performed the nanoindentation tests on an amorphous polymethymethacrylate using a holding time up to 300 s and found that the apparent stiffness is stable with increasing holding time. Geng et al. [22] used a similar indenter to test a low modulus polymer film and showed that the indentation modulus remained unchanged after a 2 s holding period. (The creep component during the initial unloading was not subtracted from the apparent stiffness in those papers). Also shown in Fig. 6 is the variation of the elastic component of the total indenter displacement (h_{max}-h_{creep}), the first term in equation (3). As expected, this term is independent of the holding time.

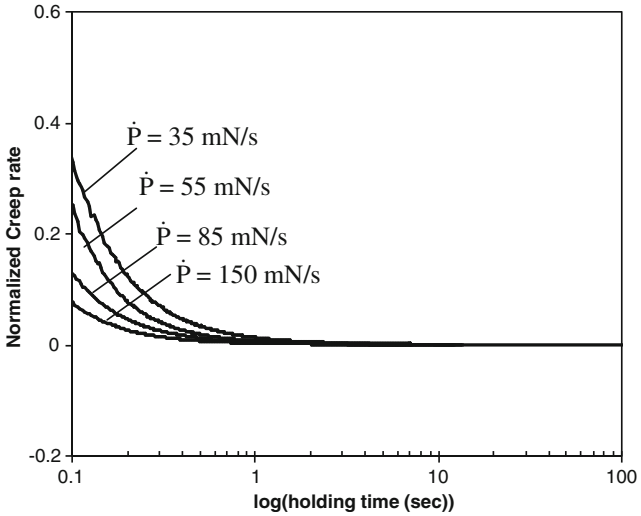

Fig. 4 Variations of creep factors (normalized creep rates) during nanoindentation of PMR-15 polyimide at ambient temperature

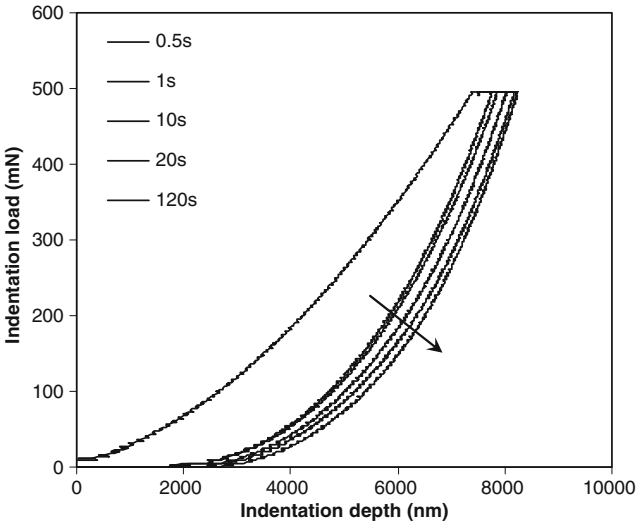

Fig. 5 Effect of holding time on indentation unloading responses of PMR-15 polyimide. The arrow points to the direction of longer holding time

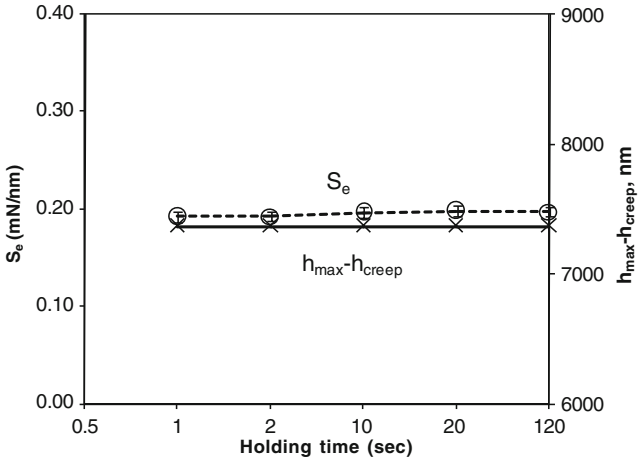

Fig. 6 Variations of elastic contact stiffness (Se) and total elastic deformation (hmax-hcreep) of PMR-15 polyimide as a function of holding time. The elastic contact stiffness (Se) was calculated using equation (2b). The unloading rate was 250 mN/s

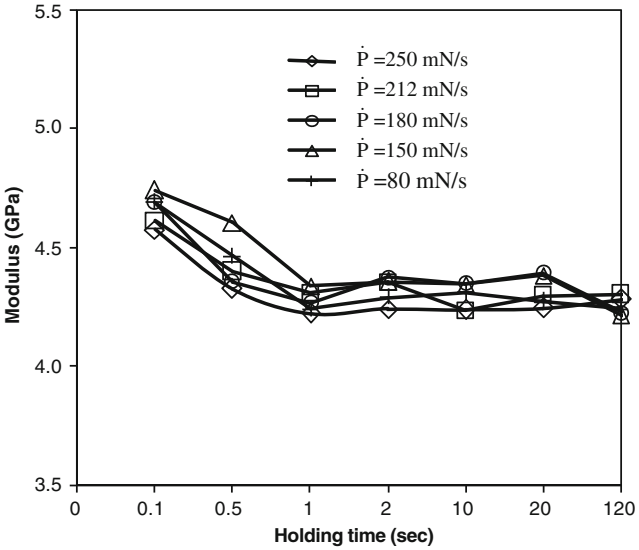

Fig. 7 Effect of holding time on elastic modulus of PMR-15 polyimide at ambient temperature

Nanoindentation of PMR-15 at Ambient Temperature

From the load-depth curves, critical parameters such as h_{max}, h_{creep}, P_{max}, $\dot{h_v}$, $\dot{P}$ and S were obtained. Substituting the information into equations (3–6), the elastic modulus and hardness of the PMR-15 were computed. Figure 7 shows the dependence of the average elastic modulus of PMR-15 on holding time. The modulus is higher initially since the creep effect is dominant at smaller holding time. Then, the modulus converges to a plateau value as the holding time is greater than approximately 1 s. Concerning all other potential effects (including the instrument drift to be discussed in later section), a 2 s holding time is deemed to be sufficient and used in subsequent experiments. The optimal holding time depends upon the material tested. In general, a stiffer polymer requires a shorter holding time.

The mechanical properties obtained from nanoindentation experiments may be affected by the surface quality of the specimen. In the current experiments, the polymer specimens were prepared by grinding papers and polishing compounds, the final polishing compound being alumina with an average particle size of 0.3 μm. The surface profile of the present PMR-15 specimen has been studied by using a White Light Interferometer (WYKO NT1100). The White Light Interferometer scans the surface of the specimen vertically and generates the surface topography in three-dimensions. By analyzing the 3D image, quantitative information about the surface can be calculated. The average roughness of the surface is approximately 170 nm. In addition to the surface imperfectness, the outer layer of the specimen may be strain hardened during sample preparation stage (the surface of the specimen is polished aggressively through various polishing compounds). All these factors can contribute to errors in estimating the true mechanical properties during nanoindentation.

In the present experiments, the indenter was programmed to cyclically load and unload into the specimen under progressively increased load, up to a maximum of 500 mN. This way, the indentation load-depth curves were recorded at various depths, as illustrated earlier in Figs. 1 and 2. From those curves, the depth-dependent elastic modulus and hardness were computed through equations (3–6). As seen in Fig. 8(a) and (b), the modulus and hardness are higher at shallower depths, and then reach plateau values at a depth greater than approximately 500 nm. The average elastic modulus and hardness determined for unaged PMR-15 resin is 4.26 GPa and 0.44 GPa, respectively, which are close with results reported in literatures (obtained by dynamic modulation method) [25, 26].

Nanoindentation of PMR-15 at Elevated Temperatures

Although a substantial body of literatures is available on nanoindentation, only a few have dealt with nanoindentation at high temperatures and the studies have been mostly concentrated on standard reference material, i.e., high purity fused silica. Beake and Smith are apparently the first who have reported the high temperature nanoindentation experiments [11]. They used a nanoindenter from Micro Materials Ltd (Wrexham, UK) to examine the mechanical properties of fused silica up to 400°C. The results show that the elastic modulus of fused silica increases by a factor of 1.1 as the temperature increases from ambient to 200°C. Schuh et al. [12] tested fused silica by using a nanoindenter from Hysitron, Inc (Minneapolis,

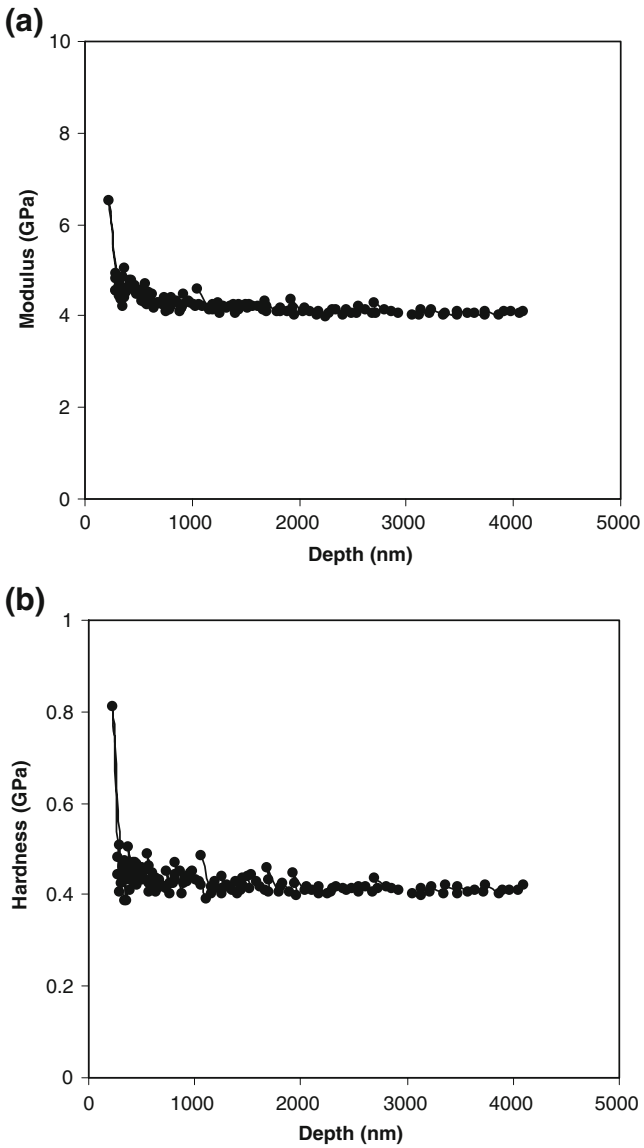

Fig. 8 (**a**) Indentation depth dependent elastic modulus of PMR-15 polyimide at ambient temperature. (**b**) Indentation depth dependent hardness of PMR-15 polyimide at ambient temperature

USA) with a self-built heating-cooling system. It is concluded that the modulus of fused silica increases by about 1% for every 100 K, or by a factor of 1.01 from room temperature to 200°C.

The current high temperature experiments were performed on a MTS Nano Indenter (Oak Ridge, TN) using XP mode. The indenter is equipped with a hot-stage heating system and a thermal-protective shield (to prevent the radiation of heat from hot-stage to indenter transducer assembly). Prior to testing PMR-15, the fused silica was examined. Figure 9 shows the load-depth curves of fused silica tested from 120°C to 240°C. It is observed that there is negligible difference in load-depth responses. Detailed calculations show that the modulus of fused silica increases

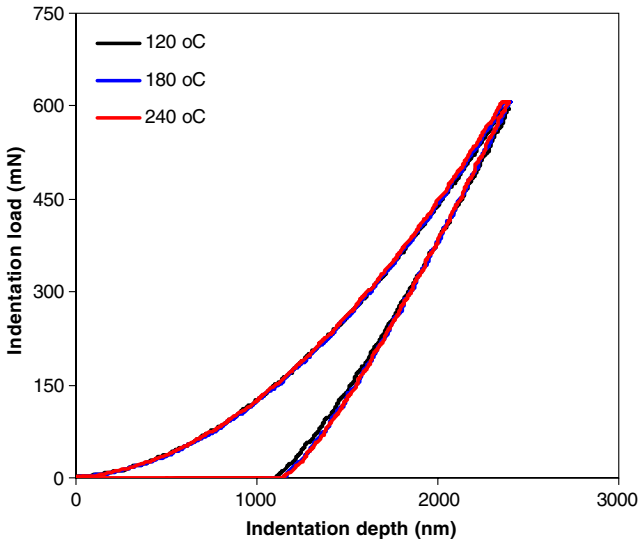

Fig. 9 Indentation load-depth curves of fused silica at elevated temperatures

by a factor of approximately 1.02 as temperature is raised from ambient to 200°C, which is consistent with the finding reported by Schuh et al. [12].

The nanoindentation tests were then performed on PMR-15 polyimide resin at elevated temperatures (50, 75, 100, 150, 200°C). A 2 s holding time derived earlier has been used for all experiments. Different holding times have been investigated at elevated temperatures and results indicate that a 2 s holding period seems to be sufficient for minimizing the creeping effect on initial unloading response (Fig. 10). Holding the indenter for a longer time at elevated temperature may not be beneficial since it may introduce additional errors due to the presence of thermal

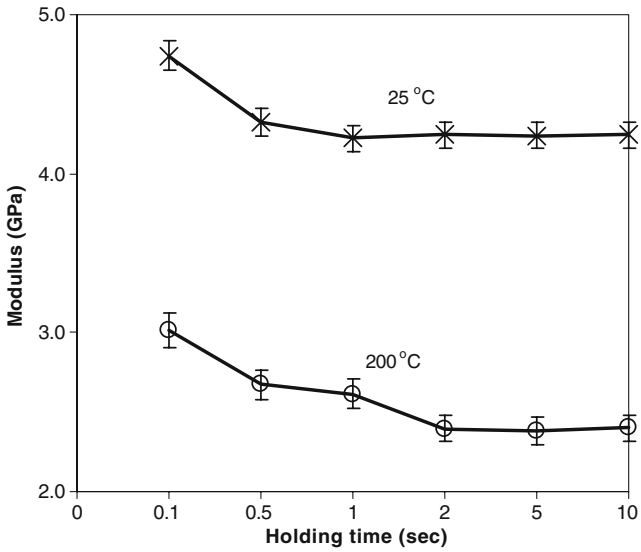

Fig. 10 Effect of holding time on elastic modulus of PMR-15 polyimide at 200°C

drift. In a high temperature nanoindentation experiment, the potential sources of thermal drift may include the thermal expansion of indenter tip, the transient thermal contraction at tip-specimen interface, and electric drift of the sensing and actuating devices. Over a longer period of holding time, these potential drifts may cause additional movements at the indenter tip and thus affect the indentation response. The drift effect becomes evident on the creep curve of PMR-15 at 200°C as recorded during indenter holding time segment (Fig. 11). Compared to the smooth creep curve obtained at ambient condition, the creep curve at 200°C is much nosier, showing signs of both expansions/contractions due to various sources of thermal drifts.

Figure 12 shows the indentation loading-unloading responses of PMR-15 at elevated temperatures (50–200°C). The load-depth curve becomes less stiff as temperature increases. Following the same analysis procedures used in room temperature experiments, the elastic modulus and hardness were computed. A total of 36 measurements were conducted at each temperature on two separate specimens. Measurements obtained at each testing condition are consistent and the amount of error (deviation) is small. This indicates that the current high temperature nanoindentation technique is reliable for quantitative characterizations of local material properties at elevated temperatures.

Finally, the average elastic modulus of unaged PMR-15 resin obtained from nanoindentation tests is plotted as a function of temperature, as shown in Fig. 13. Also shown in the figure are the temperature-dependent elastic moduli of the same PMR-15 resin obtained from conventional tension and compression tests. The overall trend from nanoindentation test is consistent with those from macroscopic tests. It is noticed that the polymer resin has slightly higher modulus under compressive mode. This is likely a result of the hydrostatic component of the stress field when the specimen is under compression, since the mechanical properties of polymers are known to be pressure dependent [27].

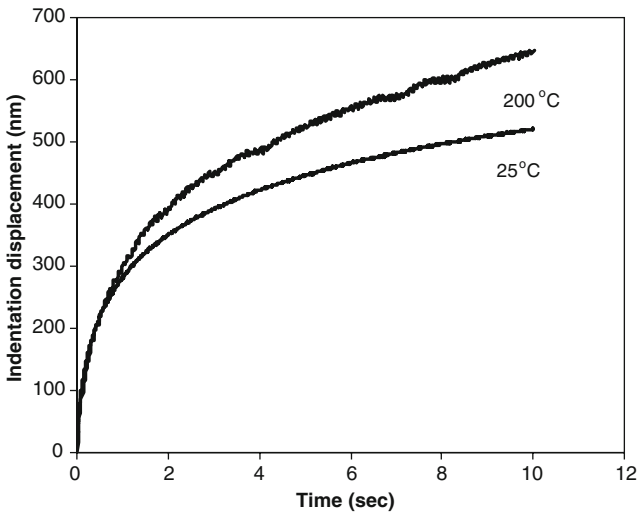

Fig. 11 Creep responses of PMR-15 during indenter holding segment (t=10 s)

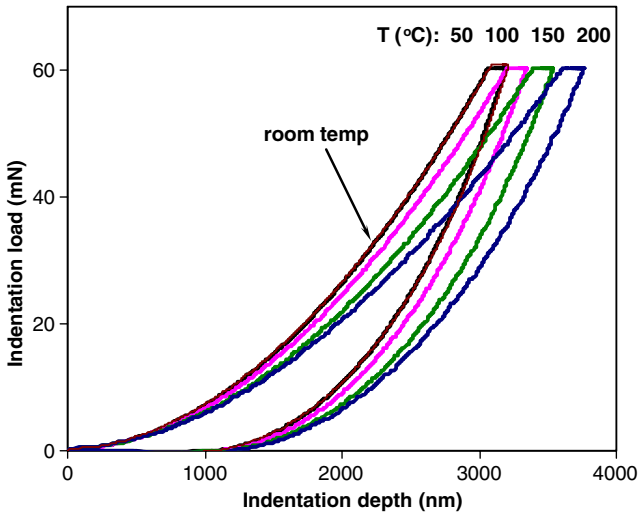

Fig. 12 Indentation load-depth curves of PMR-15 polyimide at elevated temperatures

Conclusions

The high temperature nanoindentation tests have been performed on PMR-15 polyimide neat resin using a

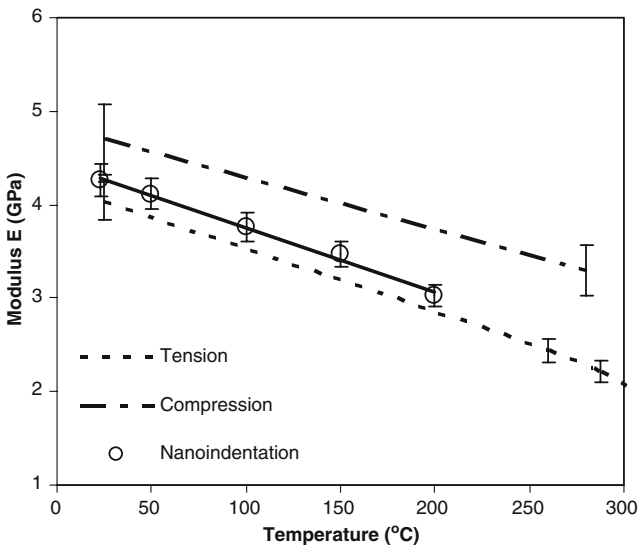

Fig. 13 Temperature-dependent elastic modulus of PMR-15 polyimide obtained from high temperature nanoindentation. The dashed lines shows the temperature-dependent Young's modulus obtained from conventional tension and compression tests

nanoindenter equipped with a hot-stage heating system. The indenter has been programmed to perform the "hold-at-the-peak" experiments using various indenter holding times and unloading rates. The normalized creep rate, a measure of creep effect, decreases with increasing indenter holding time and/or unloading rate. Analytical procedure has been modified to take into account the holding time and unloading rate so that the correct contact depth, along with elastic modulus and hardness, can be calculated. The effective holding time has been determined for the present PMR-15 at both ambient and elevated temperatures.

The high temperature mechanical properties of PMR-15 neat resin have been examined with the nanoindenter up to 200°C. Overall, the results follow the same trend as data obtained from macroscopic tests. Statistical analysis reveals that the variations in nanoindentation measurements performed at elevated temperatures are at a minimum. It thus indicates that the current high temperature nanoindentation technique is reliable for quantitative characterizations of mechanical properties of polymers/composites at elevated temperatures.

Acknowledgements This work was partially supported by the American Society of Engineering Education–Summer Faculty Fellowship Program (SFFP) and performed under the direction of Dr. Greg A Schoeppner of Air Force Research Laboratory (AFRL), WPAFB.

References

1. Oliver WC, Pharr GM (1992) An improved technique for determining hardness and elastic modulus using load and displacement sensing indentation experiments. J Mater Res 7:1564. doi:10.1557/JMR.1992.1564
2. Oliver WC, Hutchings R, Pethica JB (1986) In: Blau BJ, Lawn BR (Eds) Microindentation Techniques in Materials Science and Engineering, ASTM 889 47
3. Pharr GM, Harding DS, Oliver WC (1994) Measurement of fracture toughness in thin films and small volumes using nanoindentation methods, materials research society symposium
4. Pharr GM, Oliver WC, Brotzen FR (1992) On the generality of the relationship among contact stiffness, contact area, and elastic modulus during indentation. J Mater Res 7:613–617. doi:10.1557/JMR.1992.0613
5. Doerner MF, Nix WD (1986) A method for interpreting the data from depth-sensing indentation instruments. J Mater Res 4:601–609. doi:10.1557/JMR.1986.0601
6. Oliver WC, Pharr GM (2004) Measurement of hardness and elastic modulus by instrumented indentation: advances in understanding and refinements to methodology. J Mater Res 19:3–20. doi:10.1557/jmr.2004.19.1.3
7. Lu YC, Shinozaki DM (1998) Deep penetration micro-indentation testing of high density polyethylene. Mater Sci Eng A 249:134–144. doi:10.1016/S0921-5093(98)00571-1
8. Huang G, Wang B, Lu H (2004) Measurements of viscoelastic functions of polymers in the frequency domain by nanoindentation. Mech Time-Depend Mater 8:345–364. doi:10.1007/s11043-004-0440-7
9. Odgeard GM, Bandorawalla T, Herring HM, Gates TS (2002) Characterization of viscoelastic properties of polymeric materials through nanoindentation, Experimental Mechanics
10. Lu H, Wang B, Ma J, Huang G, Viswanathan H (2003) Measurement of creep compliance of solid polymers by nanoindentation. Mech Time-Depend Mater 7:189–207. doi:10.1023/B:MTDM.0000007217.07156.9b
11. Beake BD, Smith JF (2002) High-temperature nanoindentation testing of fused silica and other materials. Philos Mag A 82:2179
12. Schuh CA, Packard CE, Lund AC (2006) Nanoindentation and contact-mode imaging at high temperatures. J Mater Res 21:725–736. doi:10.1557/jmr.2006.0080
13. Volinsky AA, Moody NR, Gerberich WW (2004) Nanoindentation of Au and Pt/Cu thin films at elevated temperatures. J Mater Res 19(9):2650–2657. doi:10.1557/JMR.2004.0331
14. Sawant A, Tin S (2008) High temperature nanoindnetation of a Re-bearing single crystal Ni-base superalloy. Scr Mater 58:275–278. doi:10.1016/j.scriptamat.2007.10.013
15. Schoeppner, GA, Tandon GP, Pochiraju KV (2008) Predicting thermo-oxidative degradation and performance of high temperature polymer matrix composites. in Multiscale Modeling and Simulation of Composite Materials and Structures, Kwon Y, Allen D, Talreja R (Eds), ISBN**:** 978-0-387-36318-9, Springer Verlag.
16. Putthanarat S, Tandon GP, Schoeppner GA (2008) Influence of aging temperature, time, and environment on thermo-oxidative behavior of PMR-15: Nanomechanical characterization. J Mater Sci 43:6714–6723. doi:10.1007/s10853-008-2800-1
17. Meador MAB, Lowell CE, Cavano PJ, Herrera-Fierro P (1996) On the oxidative degradation of nadic endcapped polyimides: I. effect of thermocycling on weight loss and crack formation. High Perform Polym 8:363–379. doi:10.1088/0954-0083/8/3/003
18. Data Sheet Cytec Engineered Materials.http://www.cytec.com/engineered-materials/products/Cycom2237.htm, Greenville Texas.
19. Ngan AHW, Tang B (2004) Viscoelastic effects during unloading in depth-sensing indentation. J Mater Res 17(10):2604–2610. doi:10.1557/JMR.2002.0377
20. Briscoe BJ, Fiori L, Pelillo E (1998) Nano-indentation of polymeric surfaces. J Phys, D, Appl Phys 31:2395–2405. doi:10.1088/0022-3727/31/19/006
21. Cheng YT, Cheng CM (2005) Relationships between initial unloading slope, contact depth, and mechanical properties for conical indentation in linear viscoelastic solids. J Mater Res 20 (4):1046–1052. doi:10.1557/JMR.2005.0141
22. Geng K, Yang F, Grulke EA (2008) Nanoindentation of submicron polymeric coating system. Mater Sci Eng A 479:157–163. doi:10.1016/j.msea.2007.06.042
23. Mayo MJ, Siegel RW, Liao YX, Nix WD (1992) Nanoindentation of nanocrystalline ZnO. J Mater Res 7:973–979. doi:10.1557/JMR.1992.0973
24. Cheng Y-T, Cheng C-M (2001) Scaling relationships in indentation of power-law creep solids using self-similar indenters. Philos Mag Lett 81:9–16. doi:10.1080/09500830010008457
25. Putthanarat S, Tandon GP, Schoeppner GA (2007) Influence of polishing time on thermal-oxidation characterization of isothermoally aged PMR-15 resin. Polym Degrad Stab 92:2110–2120. doi:10.1016/j.polymdegradstab.2007.07.007
26. Johnson LL, Eby RK, Meador MAB (2003) Investigation of oxidation profile in PMR-15 polyimide using atomic force microscope (AFM). Polymer 44:187. doi:10.1016/S0032-3861(02)00726-7
27. Young RJ, Lovell PA (1991) Introduction to Polymers, 2nd edn. CRC, New York